Role of oxidation in aluminium foams blown by external gas injection

N. Babcsán[1,2], F. Garcia-Moreno[1,2], J. Banhart[1,2]

[1]*Hahn-Meitner-Institut Berlin, Departement of Materials Science, SF3, Glienicker Straße 100, 14109 Berlin, Germany*
[2]*Technical University Berlin, Institute of Materials Sciences and Technology, Hardenbergstr. 36, 10623 Berlin, Germany*

Liquid metal foams were produced or attempted to produce by injecting gas into three different conditioned aluminium-based melts. First into a Duralcan F3S20S composite melt (yielding what is known as "Metcomb" foams), second into a melt pre-treated with oxygen (of the type used for making "Alporas" foams), third into melted compacted powders. In all cases some foam could be produced, but quality varied.

Foam generation and decay was examined in-situ by X-ray radioscopy using a micro-focus X-ray source. For Metcomb-type foams drainage and accumulated rupture events were quantified for different oxygen partial pressures of the foaming gas.

Comparing foamability of the different foams we found that it increased from the molten powder compact to the melts pre-conditioned by oxidation and finally to the composite melts. Here the overall porosity of the foam and uniformity of cells served as criteria. Foams from Duralcan melts can be further stabilized using blowing gases containing oxygen. Increasing partial pressure of oxygen decreased both rupture of cell walls and drainage.

Keywords: metallic foam, foam stability, oxygen, X-ray radioscopy

Introduction

Metal foams belong to the class of the cellular materials which have a number of promising application [1, 2]. Several process routes exist to produce them but all products suffer from imperfections originated during foam evolution. The production routes can be classified based on the source of the gas. Thus, we distinguish between external gas injection and the route where internal gas sources are used [3]. The quality of the foam depends on the foam homogeneity reached during foam formation but strongly influenced by rupture and drainage during foam decay. In external gas injection the formation and decay can be separated more easily while the blowing agent addition leads to foam evolution where these two phenomena are overlapped. In this paper we are focusing on foam life after foam formation in case of external gas injected foams.

Metal foam production requires the present of solid inclusion [4, 5]. In order to eliminate rupture of cell walls and drainage of liquid the foam stability has to be improved. An oxide skin can further stabilize metal foams [6] leading to permanently stable foam, without oxide skin formation only metastable foams, without particles only transient foams [7] can be made if external gas bubbling has been applied. Using internal gas sources as hydrides the blowing gas, which is hydrogen, creates bubbles without any skin. However, nearly all of the previous experiments of that type are carried out in air ambient atmosphere that is producing an outside oxidized stable foam layer [8]. Until now very few investigation has been carried out with conscious selection of the ambient gas composition. Therefore, it could not been decided yet whether the penetrating oxygen from the ambient gas or the inner oxide network itself [9] leads to the observed permanently stable foams in some cases.

Recently in situ examination of metal foam evolution by X-ray radioscopy made qualitative comparison of the evolving foams possible [10, 11]. Combination of this advanced monitoring technique with the gas injection method we aimed to quantitatively characterise rupture and drainage varying the precursor type and the oxygen concentration of both the ambient and the foaming gas.

Experiments

In this study the liquid metal foam decay of gas injection foamed aluminium melts have been investigated. The sketch of the foaming is shown in Fig.1. Foams were attempted to make from compacted powder, in situ oxidized melts and Duralcan composite of the following compositions (Table 1). Previously foam were successfully produced using TiH_2 blowing agent of the same compacted powder (Alulight type) and oxidized melts (Alporas type) indicating that the precursors contained sufficient amount of oxide inclusions.

We produced the foams in BN coated foaming cartridge using a preciously controlled X-ray transparent furnace of ADMATIS Ltd. [12] by external gas injection.

Table 1. Composition of the precursors

	Matrix composition	Solid inclusions
Compacted powder	Al alloy with 7 wt.% Si	Oxide remnants
Oxidized melt	Al alloy with 3 wt% Ca	Oxide bifilms
Duralcan MMC, F3S20S	Al alloy with 9 wt.% Si and 0.6 wt.% Mg	20 vol.% of SiC particles of 10 μm size

With an appropriate foam generator approximately 6 mm diameter bubbles were created in the melts during a 5 s period while the bubbles rose to the top of the melt creating

a foam. The melt temperature was kept constant (700°C) during foam formation and up to 5 min of the following isothermal holding (Fig. 2).
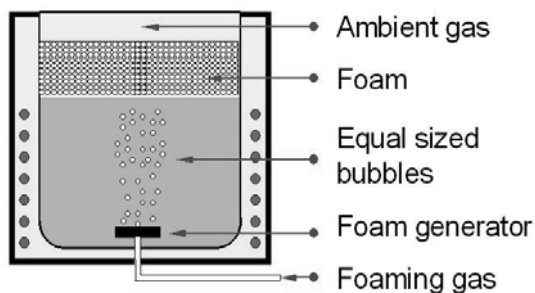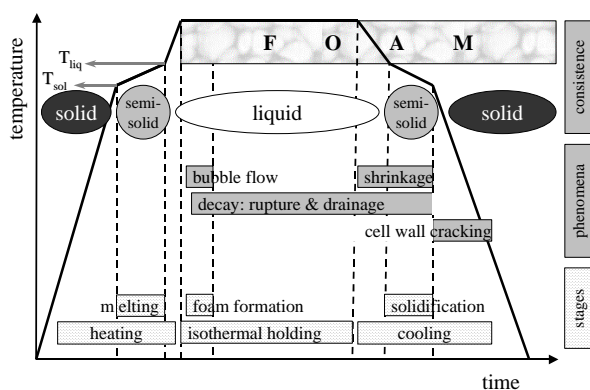

Fig.1. Sketch of the foaming process

Fig. 2. Scheme of foam evolution during the experiments

In the first series of experiments air was blown into all of the three melted precursors which were surrounded by air ambient gas. In the second series argon gas with 0.02 vol. % of oxygen was blow into liquid Duralcan MMC in air ambient atmosphere. In the third series different oxygen concentration of the foaming gases were applied making foams from Duralcan MMC mels in argon ambient gas containing 0.02 vol. % oxygen (Table 2).

Table 2. Composition of the applied gases

	1st series	2nd series	3rd series
Ambient gas	Air	Air	Argon + 0.02 vol. % O$_2$
Foaming gases			
Compacted powder	Air		-
Oxidized melt	Air		-
Duralcan MMC, F3S20S	Air	Argon + 0.02 vol. % O$_2$	Argon + 0.02, 0.16, 0.85. 1.5, 8.5, 100 vol. % O$_2$

The foam evolution has been monitored by X-ray radioscopy using microfocus X-ray source and panel detector described in previous publication [11]. Two panel detector have been used one in fast (25 fps) and the other in normal mode (1 fps). For evaluation of the rupture events and the drainage image analysis software called AXIM has been used [11].

Results and Discussion

Effect of the precursor

In the first series of experiment the different air foamed precursors have shown significant variation on foam architecture (Fig. 3). The bubbles of melted powder compact even collapsed during foam formation and only dross like structure was created (Fig. 3a). Some of the bubbles, which were injected into the oxidized melt, remained stable during isothermal holding while the rest collapsed leaving an onion shape structure on the top (Fig. 3b). The SiC particles stabilized melt was good foamable resulted in stable monodisperse foam (Fig. 3c).
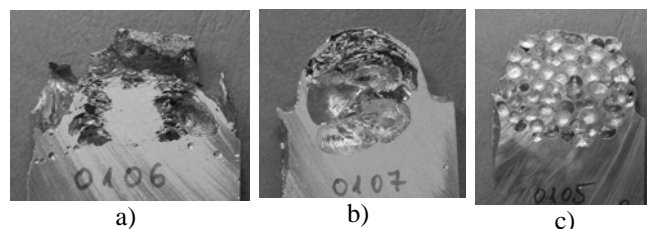

Fig. 3. Architecture of foams made of different precursors blowing air into the melt: a) compacted powder, b) oxidized melt and c) Duralcan MMC foam width is 40 mm

Recent publication of Körner et al. [9] revealed the distribution of oxide remnants in the powder compact foams which thought to play important rule on foam stability. It was shown that the remnants didn't segregate on the surface but distribute homogeneously. The remnant structure can be considered as a gel network of colloid systems [3]. It has also been reported [9] that the mixing or bubble flow destroys this oxide remnant network leaving agglomerated superparticles in the cell walls or Plateau borders. Therefore it is in hand that the external gas injection is too harmful process that creates more shearing effect than could be withstand by the network. The microstructure of oxidised melt (Alporas type foams) [6] consists of loosely connected oxide bifilms which have larger size than the oxide remnants. In this case also the lack of surface segregation reported [6]. In the third case SiC particles segregates on the surface of the foams [13]. This behaviour can lead to the best stability during bubble movement creating exceptional quality metal foams. The resulted architectures made of the different precursors

indicate that the rheological behaviour therefore foam stability during foam formation improving in the following order: powder compact, oxidised melt and MMC melt.

Effect of ambient atmosphere

It was shown previously that the oxygen concentration of ambient gas affects expansion of powder compacts blown by hydrides, using air ambient gas the expansion of the foam has been reduced compared to argon [8]. In case of gas injected foams the nitrogen blowing resulted metastable foams with a coarse architecture and partially ruptured cell walls if the ambient gas was air [13]. We repeated this latter experiment with argon blowing gas (oxygen 0.02 vol. %) and air ambient gas. Several holes could have been observed on the surface of the foam (Fig. 4a). These holes are situated in the middle of the cell walls probably where the thickness of the foam was the least (Fig. 4b).
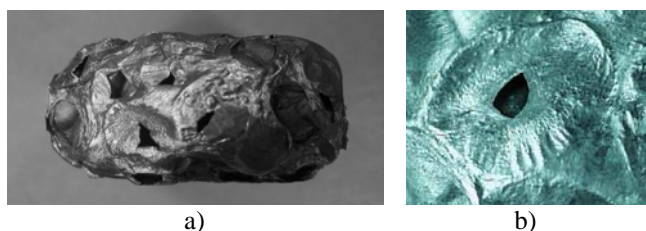

a)   b)

Fig. 4. Macroscopic images of stopped rupture of a cell wall of Duralcan MMC due to penetrating oxygen caused stabilization from the ambient gas: a) top view of a foam sample, b) frozen rupture of one cell wall.

The rupturing time of the cell walls was in situ monitored by the X-ray radioscopy. The images (Fig. 5) were taken from a position which was close to the melt surface and far from the top of the foam to eliminate the effect of the ambient gas oxygen content. The lines correspond to Plateau borders in the figures. The time difference and the exposition time were set to 40 ms and 33 ms respectively in the subsequent images. In Fig. 5 two rupturing events can be observed. The first slowly disappear in Fig. 5b and the second in Fig. 5c. From this observation it can be stated that the rupturing time in the range of the exposition time This value is in a good agreement of previous study made by synchrotron radioscopy where an upper limit of 55 ms [14].

The accumulated values of rupturing events are plotted in the function of time in Fig. 6. The foam formation finished at 22 s but 26 s incubation time needed until the ruptures were started. After 130 s no more ruptures occur saturation takes place due to the oxygen penetration in to the foam cells through rupture holes (Fig. 4b). It can be seen that some extra rupture happens during solidification around 400 s.
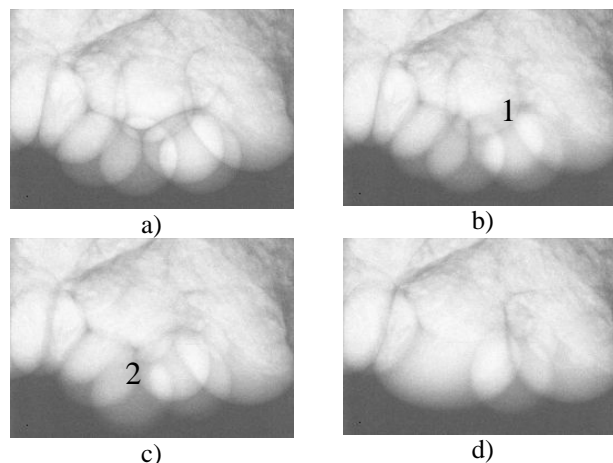

a)   b)

c)   d)

Fig. 5. Fast X-ray images of a rupture event in foam made of Duralcan MMC blown with argon (0.02 vol. % O_2). The exposition time of the individual images was set to 33 ms with 25 frames being recorded per sec. Width of each image is 14 mm.
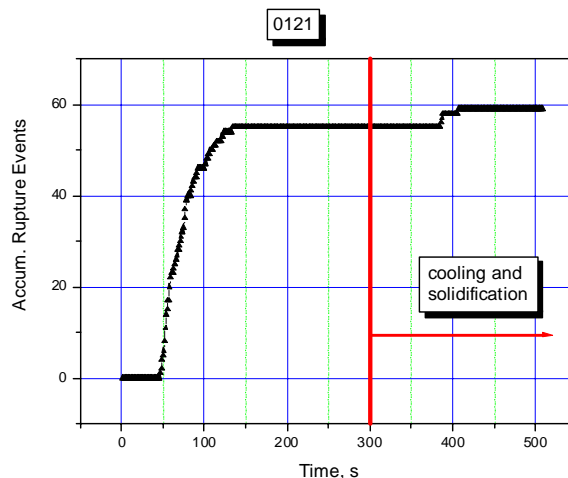

Fig. 6. Accumulated rupture events diagram of foamed liquid Duralcan MMC with high purity argon foaming gas (oxygen 0.02 vol. %) in air ambient gas.

Effect of the foaming gas

For investigating the effect of foaming gas on the stability of the metal foams high purity ambient argon atmosphere (oxygen less than 0.02 vol. %) has been selected. Therefore no saturation occurred due to penetrating oxygen from the ambient gas. The foaming gas oxygen content varied between 0.02 and 100 vol.%. Rupture and drainage are strongly appearing on the subsequent images of foam evolution using 0.02 vol. % oxygen containing argon gas (Fig. 7).
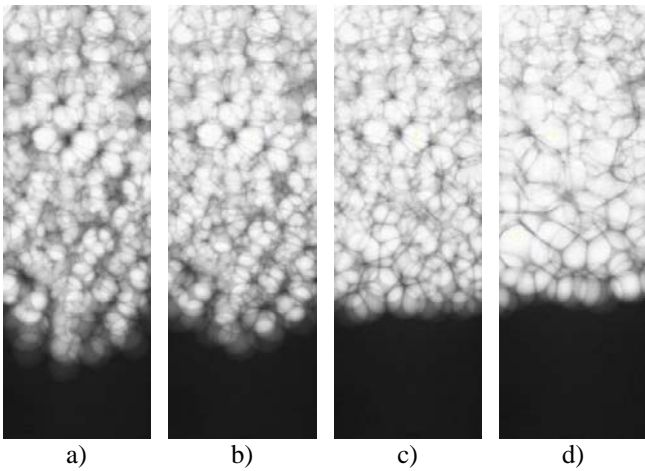
Fig. 7. X-ray radiographs of liquid metal foams of Duralcan MMC blown with argon containing *0.02 vol. %* of oxygen, after a) 0s, b) 100s, c) 200s and d) 500 s isothermal holding, image width is 26.5 mm.

Contrary the rupture of the foam cells are hardly visible and only a slight liquid level increasing occurred if the oxygen concentration reaches 8.5 vol. % (Fig. 8). Thus, the accumulated rupture events were calculated in foams containing argon + 0.02, 0.16, 0.85, 1.5, 8.5 vol. % O_2 respectively (Fig. 9). No rupture was detected when 100 vol. % oxygen has been used. Most probably the oxide skin reached a value where the strength of the skin is higher than the stress caused by the liquid movement of surface waves. We have to note that air foaming gas, which corresponds to 21 vol. % oxygen, results also permanently stable foam without any rupture event [15].
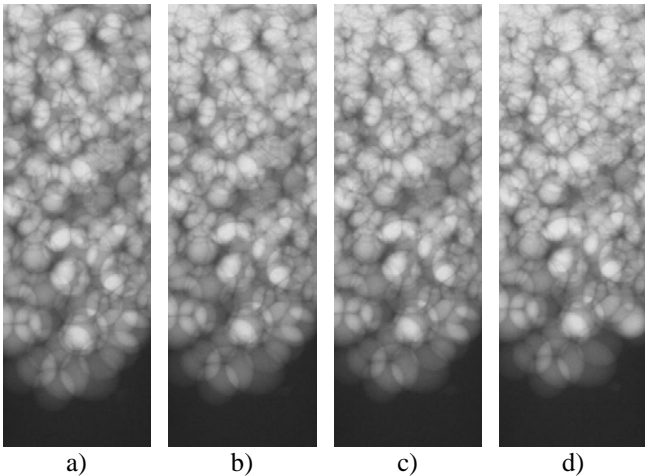

Fig. 8. X-ray radiographs of liquid metal foams of Duralcan MMC blown with argon containing *8.5 vol. %* of oxygen, after a) 0s, b) 100s, c) 200s and d) 500 s isothermal holding, image width is 26.5 mm.
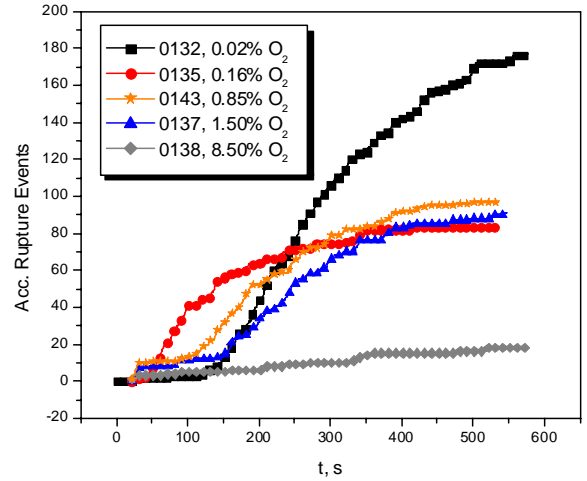

Fig. 9. Accumulated rupture events diagrams of foams made by different oxygen concentration of the foaming gases

It can be seen in Fig. 9 that not only the total number of the ruptures but also the incubation time of the first rupture varies with the oxygen concentration. A general decreasing tendency of the rupturing events can be observed by increasing oxygen concentration. Significant change occurs between 1.5 and 8.5 vol. % of oxygen concentration. It has to be noted that no saturation of the rupturing events occurred which can be originated to the low oxygen content of the ambient gas.

The plots of the spatial distribution of the rupturing events are shown in Fig. 10 and 11.
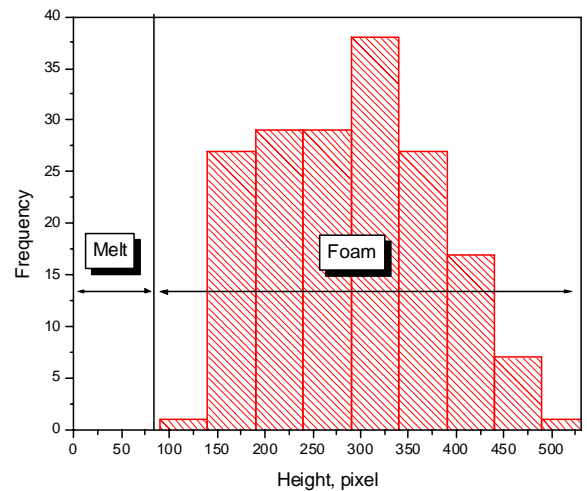

Fig. 10. Spatial distribution frequency of ruptures in foam made of Duralcan MMC with 0.02 vol. % oxygen containing foaming gas.
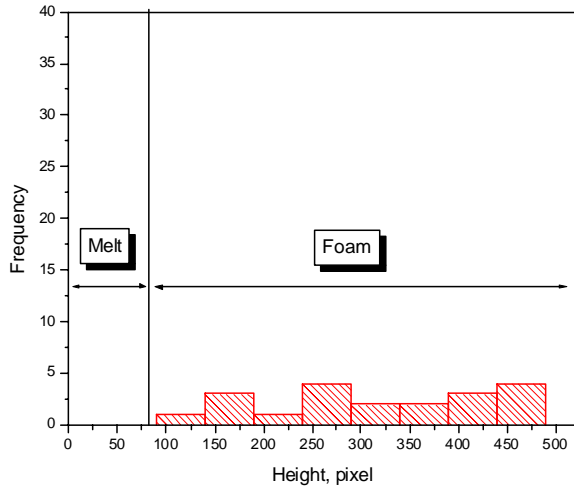
Fig. 11. Spatial distribution frequency of ruptures in foam made of Duralcan MMC with 8.5 vol. % oxygen containing foaming gas.

The spatial distribution is homogeneously distributed in both cases with a slight decrease on the top of the foam when 0.02 vol. % oxygen has been applied (Fig. 10). The reason could be that the foam takes more oxygen from the larger volume of the ambient gas chamber than from the small bubbles.

Drainage kinetics can be characterised from the density distribution curves calculated from the X-ray images by AXIM software. It can be seen that the drainage dominant at the first 200 s that slow down significantly after (Fig. 12).
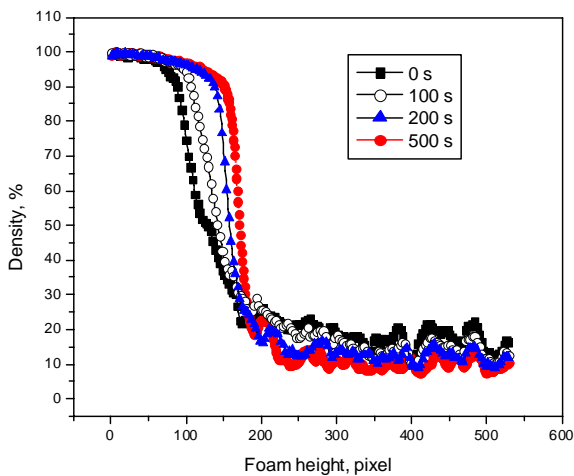

Fig. 12. Density distribution of liquid metal foams of Duralcan MMC blown with argon containing 0.02 wt.% of oxygen caculated of images in Fig. 7.

One can define the following drainage numbers from the density distribution curves (Fig. 13): Height of stationary density (h_s) is the height where the density of the foam remains constant in time. Positive drained volume (V_D^+) is the integral of the drained liquid from the bottom of the melt until h_s. Negative drained volume (V_D^-) is the integral of the draining liquid from the top of the melt until h_s. Average density (ρ_0 and ρ_{500}) is the integrate of the density between the top of the melt and h_s just after foam formation and after 500s isothermal holding respectively. Average foam density change is the difference of the two densities above.
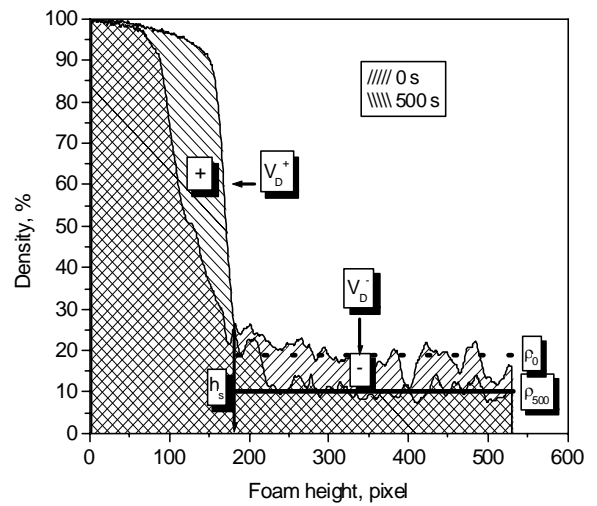

Fig. 13. Drainage numbers defined from density distribution curves just after foaming (0s) and after 500 s isothermal holding.

For comparing the effect of the oxygen concentration the average foam density changes were plotted in Fig. 14. A general decreasing tendency of the drainage with increasing oxygen content were observed.
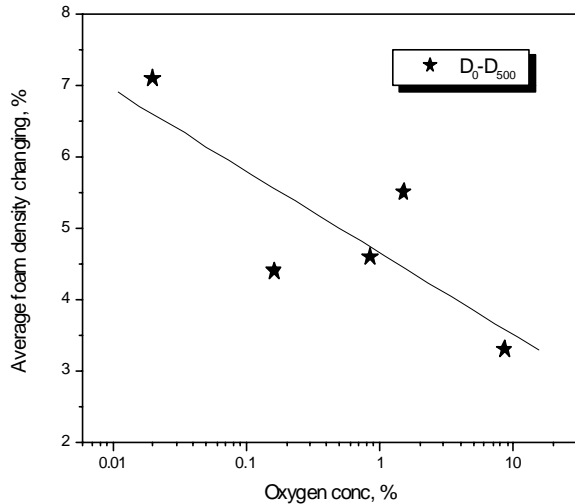
Fig.14. Average foam density changes in the function of the oxygen concentration of the foaming gas

This tendency can be explained using experimental results on single Plateau borders of Koehler et al. in aqueous foams [16].. There it was shown that the mobility of film surfaces determines the drainage rate. Immobile surfaces slow down drainage. Using the analogy with aqueous foams, the oxide can be considered as an immobiliser of surfaces, thus leading to less drainage.

Conclusion

In situ X-ray radioscopy has been used to examine monodisperse foams made by gas injections into powder compacts, oxidized melt and F3S20S Duralcan composite. Stability increased by this order. Both, ambient and foaming gas, are influencing coalescence and drainage.

Oxygen concentration of the bubbling gas decreased rupture and drainage of the liquid metal foam. Drastic changes of foam decay occurred between 1.5 and 8.5 vol. % oxygen concentration. The coalescence tendency of the foams compared quantitatively using accumulated rupture events diagrams. Drainage were characterized quantitatively based on numbers introduced as drained volume, height of stationary density, average density in the foam.

Proposed mechanism for rupture is the increase strength of the film by thicker solid oxide and damping surface waves by a particle monolayer glued to the oxide skin. Drainage is decreased by the immobilization of the surface of the cell wall similarly to the mechanism proposed in aqueous foams.

REFERENCES

1 M.F. Ashby, A. G. Evans, J. W. Hutchinson and N. A. Fleck: *Metal Foams - a design guide*, (Butterworth-Heinemann 2000)
2 J. Banhart: Progress in Materials Science 46 (2001) 559-632
3 N. Babcsán and J. Banhart: Metal foams towards high-temperature colloid chemistry in *Colloidal Particles at Liquid Interfaces*, ed. by B.P. Binks and T.S. Horozov, (Cambridge University Press, in press)
4 N. Babcsán, D. Leitlmeier and H. P. Degischer: Materialwissenschaft und Werkstofftechnik 34 (2003) 22-29
5 N. Babcsán, D. Leitlmeier and J. Banhart: Colloids and Surfaces A, 261 (2005) 123-130
6 N. Babcsán, D. Leitlmeier, H.-P. Degischer, J. Banhart: Adv. Eng. Mat. 6 (2004), 421-428
7 R.J. Pugh: Adv. in Coll. and Int. Sci., 64 (1996) 67-142
8 F. García-Moreno, N. Babcsán and J. Banhart: Colloids and Surfaces A. 263 (2005) 290-294
9 C. Körner, M. Arnold and R.F. Singer: Mat. Sci. and Eng. A, 396 (2005) 28-40
10 J. Banhart, H. Stanzick, L. Helfen and T. Baumbach: Applied Physics Letters, 78 (2001) 1152-1154
11 F. Garcia-Moreno, M. Fromme, J. Banhart: Adv. Eng. Mat. 6 (2004) 416-420
12 www.admatis.com
13 N. Babcsán: *Ceramic Particle Stabilized Aluminum Faoms*, Ph.D. thesis, (University of Miskolc, Hungary, 2003)
14 H. Stanczik, M. Wichmann, J. Weise, L. Helfen, T. Baumbach, J. Banhart: Adv. Eng. Mat., 4 (2002) 814-823
15 N. Babcsán, F. García-Moreno, D. Leitlmeier and J. Banhart: Materials Science Forum, in press
16 S.A. Koehler, S. Hilgenfeldt, E.R. Weeks and H.A. Stone: Phys. Rev. E, 66 (2002) 040601